ExHFT-7
28 June – 03 July 2009, Krakow, Poland

THE EFFECT OF VELOCITY RATIO ON THE THERMAL-HYDRAULIC PERFORMANCE OF RECIPROCATING SCRAPED SURFACE HEAT EXCHANGERS AT LOW REYNOLDS NUMBER

J. P. Solano[1,*], A. García[1], P.G. Vicente[2], A. Viedma[1]
[1]Universidad Politécnica de Cartagena, Murcia, Spain
[2]Universidad Miguel Hernández, Elche, Spain

ABSTRACT. The thermal-hydraulic performance of a reciprocating scraper inserted in a round tube at low Reynolds number is studied. Pressure drop and heat transfer characteristics have been experimentally determined in static conditions in laminar regime (Re_h=30), and results are contrasted with dynamic performance at several velocity ratios (ω=0.1 - 1). Maximum increases of Fanning friction factor of the order of 1.2 have been found, together with increases in Nusselt number of the order of 2, using propylene-glycol as working fluid.

Keywords: heat transfer enhancement, pressure drop, SSHE, fouling

INTRODUCTION

Heat transfer processes in the food and chemical industries frequently deal with highly viscous liquids. The performance of heat exchangers working under these conditions is usually low, as a result of the characteristics of the encountered laminar regime [1]. Moreover, the heat transfer surfaces may become coated with a deposit of solid material after a period of operation. This phenomenon, known as fouling, causes a reduced overall heat transfer coefficient [2]. Heat exchangers are generally over-designed to compensate for the anticipated fouling [1]. Moreover, cleaning operations decrease equipment availability, which causes as well a considerable economic impact.

Among the several technical solutions for fouling cleaning and prevention [3], mechanically assisted heat exchangers, where a heat transfer surface is periodically scraped by a moving element, constitute a suitable solution for applications with severe tendency to fouling and low heat transfer rates. Dynamic heat exchangers with rotating scraping blades are found in commercial practice (SSHE): they prevent fouling and promote mixing and heat transfer. Many investigations have focused on these anti-fouling devices, studying flow pattern characteristics [4], their thermo-hydraulic performance [5] or scraping efficiency [6].

This work presents the study of a dynamic insert device moved alternatively along the axial direction by a hydraulic cylinder. The active insert device is made up of several semi-circular elements, which are mounted on a shaft with a pitch of 5D (Fig. 1). When inserted inside the tube,

* Corresponding author: Juan Pedro Solano
Phone: + (34)-325938, Fax: + (34)-325999
E-mail address: juanp.solano@upct.es

the device produces a double effect: the induced flow generates macroscopic displacements from the boundary layer region to the axis of the tube, increasing heat transfer, and the elements with reciprocating movement scrape the inner tube-wall, avoiding fouling. The industrial version of this device is manufactured and market by the Spanish company HRS-Spiratube.

There is empirical evidence of the heat transfer enhancement and fouling prevention of this kind of active devices. However, the authors have not found in the open literature previous works related to this type of mechanically-assisted heat exchangers.

This work presents an experimental study on the pressure drop and heat transfer characteristics of the active insert device depicted in Fig. 1. Experimental results of Fanning friction factor *f* and Nusselt number *Nu* as functions of scraping frequency are provided for Re_{Dh}=30 (laminar flow).

EXPERIMENTAL SET-UP

A schematic diagram of the experimental setup is shown in Fig. 2. It consists of two independent circuits: the main circuit, where the dynamic insert device was installed, and the secondary circuit which was used for regulating the tank temperature to a desirable value. The reciprocating movement of the inserted scraper is achieved by means of a hydraulic unit. This unit moves a double-effect cylinder over which the shaft of the insert device is mounted. Mechanical arrangement of the end-stroke connections provides the system with a movement amplitude of 10D (180 mm). All the instrumentation was connected to a HP 34970A Data Acquisition Unit.

Pressure drop tests were carried out in the hydro-dynamically developed region under isothermal conditions. The hydraulic diameter $D_h = D - d$ was used as the reference diameter to calculate all friction factors. It takes account of the presence of the shaft inside the tube, but does not consider the effect of the plugs mounted on it. Fanning coefficients f_{Dh} were determined from fluid mass flow rate and mean pressure drop measurements by means of

$$f_{Dh} = \frac{D_h}{L_p} \frac{\overline{\Delta P}}{2 \rho \, \overline{u}_f^{\,2}} \tag{1}$$

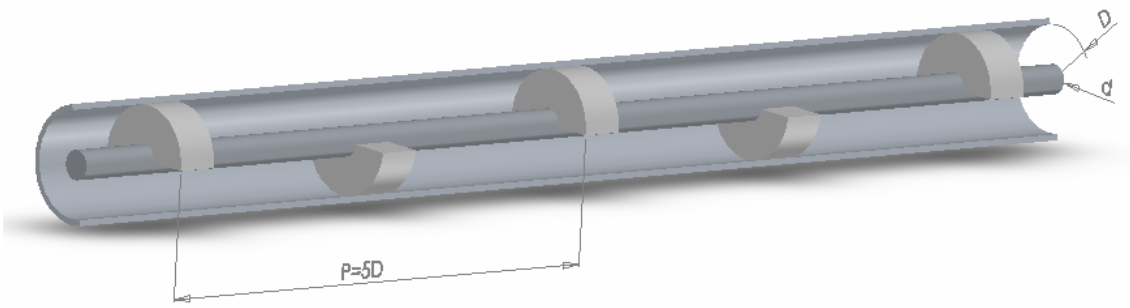

Figure 1. Sketch of the active device

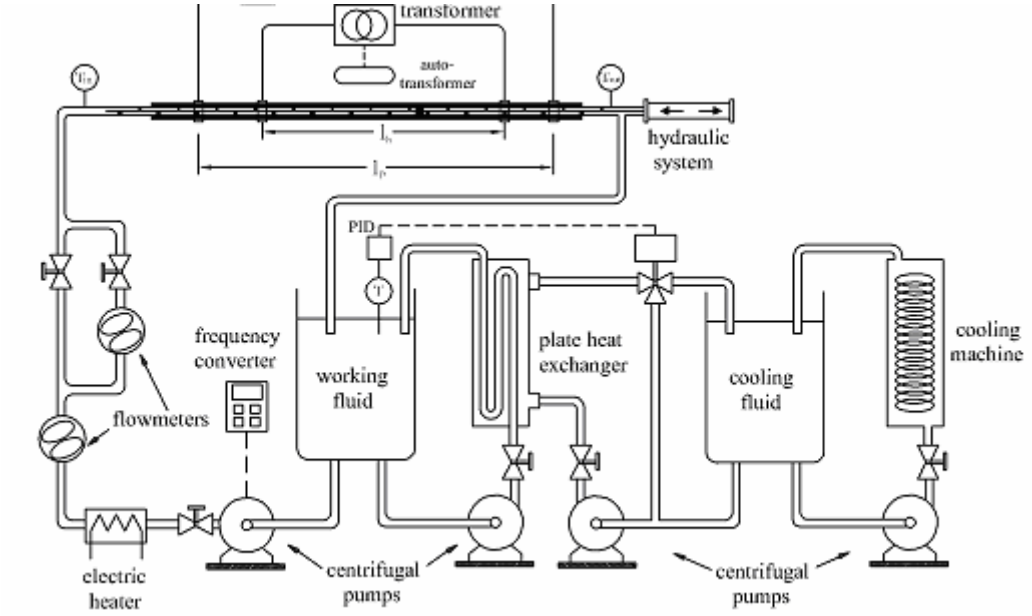

Figure 2. Experimental setup

Time-dependent pressure during the scraping process was measured in two sections of the tube separated by a distance L_p=1.8 m. Two piezorresistive pressure sensors (Kistler K-Line) were connected to each tube section with four pressure taps separated by 90º. Mean pressure drop in the tube over the scraping cycle, $\overline{\Delta P}$, was computed by integration of the instantaneous signal over 50 cycles.

Heat transfer experiments were carried out under uniform heat flux conditions, where energy was added to the working fluid by Joule effect heating. A 6 kVA transformer was connected to the smooth tube by copper electrodes and power supply was regulated by means of an auto-transformer. The length between electrodes defined the heat transfer test section (L_h = 1 m). To reduce heat losses, this section was coated with a thermal insulation of 20 mm thickness and thermal conductivity 0.04 W/mK. The overall electrical power added to the heating section, Q, was calculated by measuring the voltage between electrodes (0-15 V) and the electrical current (0-600A).

Fluid inlet and outlet temperatures, T_{in} and T_{out} were measured by submerged type resistance temperature detectors (RTDs). Since heat was added uniformly along the tube length, the bulk temperature of the fluid at the measuring section, $T_b(x_p)$, was calculated by considering a linear variation with the axial direction. Average outside surface temperature of the wall $\overline{T}_{wo}$ was measured at six different axial positions along a scraper pitch, located at 30 diameters from the upstream electrode, that ensure fully developed flow. The value of $\overline{T}_{wo}$ at each axial position was calculated by averaging the temperatures measured with eight surface type RTDs peripherally spaced by every 45º at each axial position.

The RTD naked sensors were wrapped with ultra-thin plastic films, which assured electrical isolation. The low thickness of the film makes its thermal resistance negligible. A highly thermal-

conductive paste was spread between the tube wall and the wrapped RTD sensor. Each temperature value used for data reduction was averaged over 30 data sampled every 9 seconds.

Two calibration tests with no electrical heating were done: the first test was performed to determine heat losses in the test section Q_1 by measuring $(T_{in} - T_{out})$ at low flow rates, and the second test at high flow rates to calculate the lay-out resistances of the surface type RTDs $(T_{in} \approx T_{out} \approx \overline{T}_{wo})$.

Heat flux added to the test fluid q'' is calculated by subtracting heat losses to the overall electrical power added in the test section. The power factor was 1.0, as the copper electrodes were directly connected to the metallic tube, which is a pure resistive load. The inner wall temperature $\overline{T}_{wi}$ for each experimental point, was determined by using a numerical model that solves the steady-state, one dimensional, radial, heat conduction equation in the tube wall and insulation from the following input data: $\overline{T}_{wo}$, Q, Q_1 and $T_b(x_p)$. The local Nusselt number was calculated by means of

$$Nu_x = \frac{D_h}{k} \frac{q''}{\overline{T}_{wi} - T_b(x_p)} \tag{2}$$

Visualization experiments [7] allow to state that the flow is fully developed at few pitches (2-3 p). Thus, local Nusselt number computed with Equation (2) is a periodic value. Nusselt number results at the six axial positions were corrected by the factor $(\mu_w / \mu_b)^{0.14}$ to obtain correlations free of variable properties effects [8]. Pitch-averaged Nusselt number was obtained by averaging the six local values computed with the presented methodology.

The experimental uncertainty was calculated by following the "*Guide to the expression of uncertainty in measurement*", published by ISO [9]. Details of the uncertainty assignation to the experimental data are given by the authors in [10]. Uncertainty calculations based on a 95% confidence level showed maximum values of 4% for Reynolds number, 3.5% for Prandtl number, 6% for Nusselt number and 8% for friction factor.

RESULTS

An experimental research was carried out to assess the effect of the scraping frequency on the thermal-hydraulic behaviour of the dynamic insert device sketched in Fig. 1. Experiments were carried out employing propylene-glycol at 15ºC, with a flow rate of 150 l/h, yielding to Reynolds number Re_{Dh}=30. The scraping frequencies ranged from 0.1 to 1 Hz. The velocity ratio ω, defined as $\omega = u_{scraping}/u_{fluid,}$ was found to be an excellent non-dimensional parameter to evaluate dynamic effects. The range of velocity ratios tested was ω=[0.1 0.3 0.5 0.75 1].

Pressure drop results

Pressure drop tests were carried out under isothermal conditions, covering the wide range of velocity ratios presented above, for constant Reynolds number Re_{Dh}=30. A test in static conditions (ω=0) was also performed. Time-averaged pressure drop results were employed for computing the mean Fanning friction factor as a function of ω.

Unsteady pressure signal. Figure 3 (left) shows a detail of the pressure signals over two scraping cycles, for working conditions Re_{Dh}=30 and ω=0.3. The scraper movement in the opposite direction of the flow is called "counter-current", and the scraper movement in the same direction of the flow

is called "co-current". The signals $p_1(t)$ and $p_2(t)$ can be substracted to obtain the unsteady pressure drop in the tube section (see Figure 4, right). Resulting mean pressure drop is also depicted in this graph.

The low, constant scraping velocity generates quasi-steady flow conditions in each semi-cycle, which can allow to assess the separate performance of the dynamic device in counter-current and co-current movement.

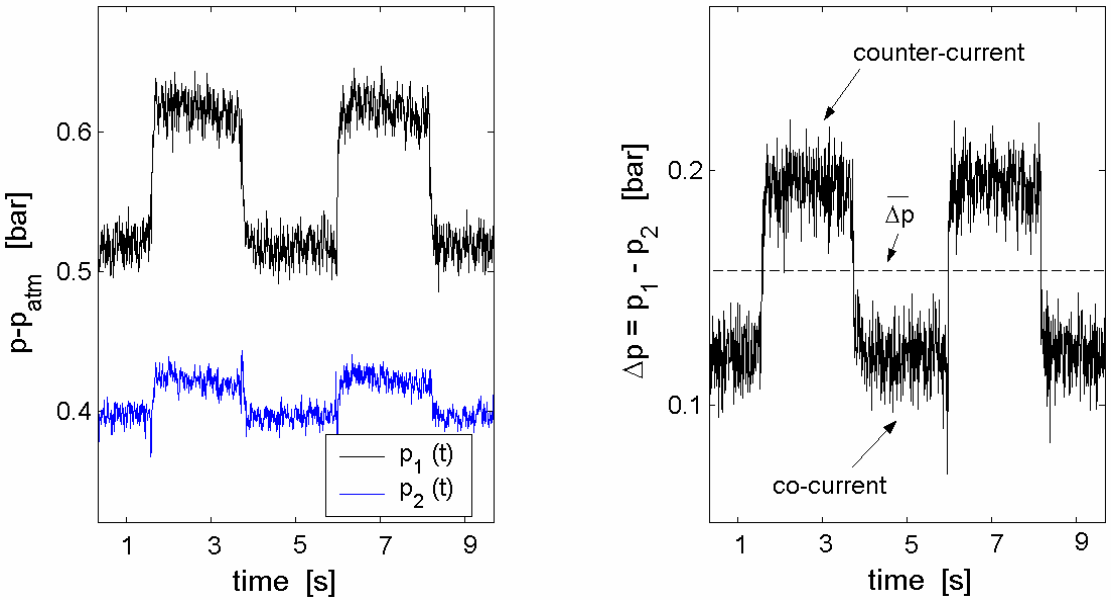

Figure 3. Unsteady pressure signal in the tube section, Re_h=30, ω=0.3

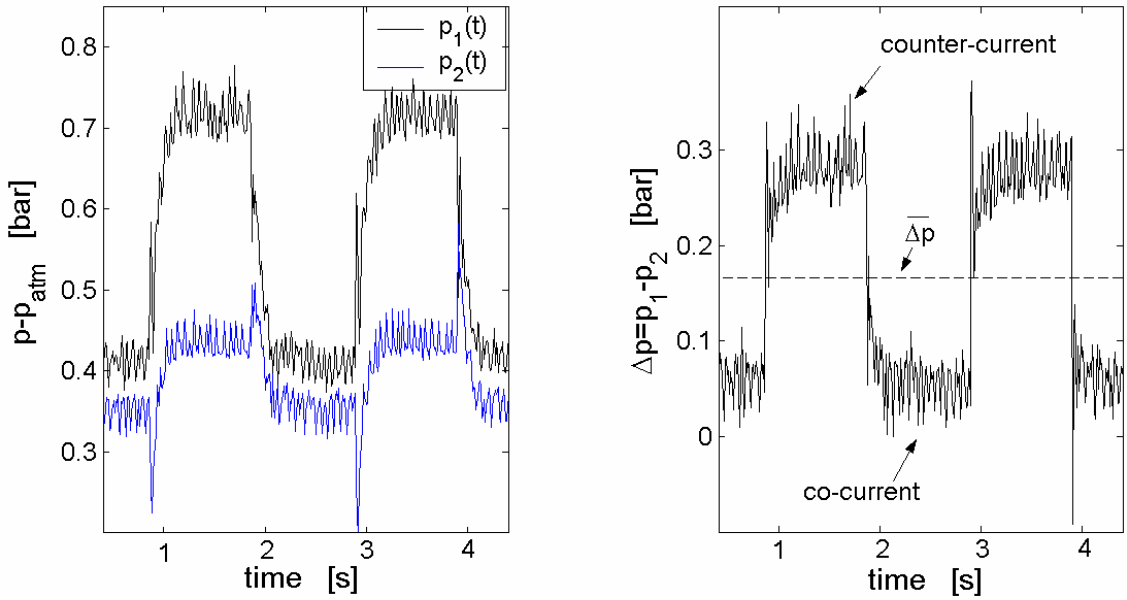

Figure 4. Unsteady pressure signal in the tube section, Re_h=30, ω=1

Counter-current performance yields to high pressure drops in the tube, as expected from the blockage effect generated by the scraper during its movement against the flow [7]. However, when the device

moves co-current, pressure drop decreases dramatically. This result reveals the lower blockage of the scraper when it moves within the flow direction.

Figure 4 shows the unsteady pressure evolution measured for the working condition Re_{Dh}=30 and ω=1. In this situation, the scraper velocity is 3.3 times higher than the velocity with ω=0.3, whereas flow rate in the tube is kept constant. Pressure drop across the tube shows transient evolutions at the commencement of each semi-cycle, as a result of the higher velocity of the scraper and the sudden movement reversal imposed by the hydraulic unit.

Pressure drop in the counter-current semi-cycle is 50% higher than for ω=0.3. Thus, scraper velocity can be stated as a remarkable factor in the increase of the blockage effect in counter-current performance. Conversely, pressure drop in the co-current semi-cycle is much lower than the equivalent result for ω=0.3. The velocity of the device in the flow direction generates a low pressure field downwards, yielding to lower pressure drops. Mean pressure drop for velocity ratio ω=1 is still higher than the corresponding value found for ω=0.3. Considering than, for higher scraping frequencies, counter-current pressure drop increases while co-current pressure drop decreases, the major influence of the counter-current characteristics in the global performance of the dynamic device can be assessed.

Fanning friction factor. The value of $\overline{\Delta P}$ for each velocity ratio can be employed to compute the mean Fanning friction factor, as explained in Equation 1. Experimental results for the range of interest are presented in Figure 5. Fanning friction factor results can be employed to estimate the pressure drop augmentation due to the insertion of the scraping device in a smooth tube with similar mass flow rate. This augmentation can be computed in laminar regime as follows:

$$\frac{\Delta P_{scraping}}{\Delta P_{smooth}} = f_{Dh} \times \frac{\mathrm{Re}_{Dh}}{16} \times \frac{D^4}{D_h^{\,3}\left(D+d\right)} \tag{3}$$

According to this expression, pressure drop increases of 5.7 have been found in static conditions, referred to the smooth tube $\left(\Delta P_{\omega=0}/\Delta P_{smooth}\right)$. In dynamic conditions, mean Fanning friction factor increases for higher velocity ratios. Pressure drop augmentation in the inserted tube due to the movement of the scraper with ω=0.1 is $\Delta P_{\omega=0.1}/\Delta P_{\omega=0}$ =1.06, while the increase due to the movement of the scraper at a velocity ten times higher (ω=1) is $\Delta P_{\omega=1}/\Delta P_{\omega=0}$ =1.21.

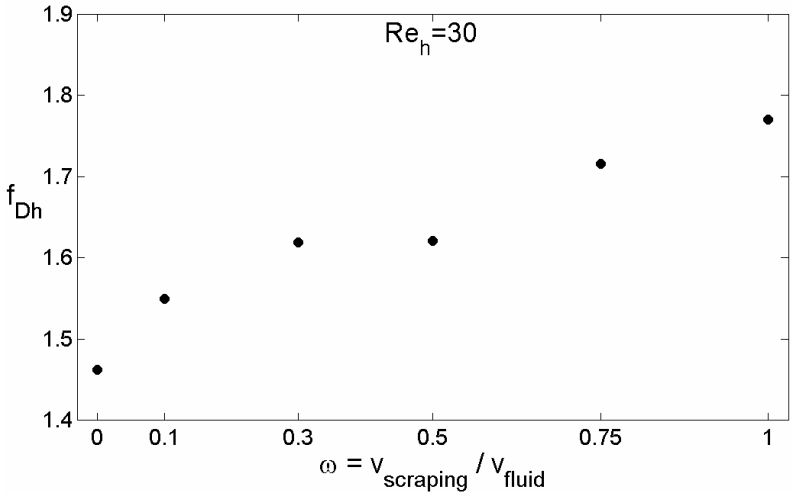

Figure 5. Mean Fanning friction factor as a function of velocity ratio (Re_{Dh}=30)

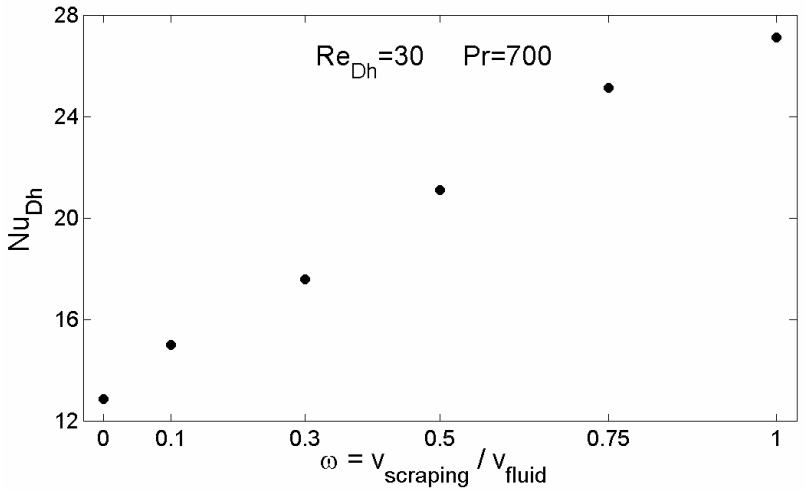

Figure 6. Mean Nusselt number as a function of velocity ratio (Re_{Dh}=30)

Heat transfer results

Heat transfer tests were performed under uniform heat flux conditions, for Re_{Dh}=30 and similar velocity ratios than in the previous section. Prandtl number was Pr=700, using propylene-glycol as working fluid at T=15ºC.

The insertion of the scraper in a smooth tube, working in static conditions, yields to heat transfer augmentations of 4.1 (referred to the asymptotic solution $Nu_{D,\infty}$=4.36). The mixing promoted by the insert device plays an essential role in this result. The effect of scraping movement increases heat transfer characteristics. For velocity ratio ω=0.1, heat transfer augments 1.35 times with respect to the static conditions. The continuous removal of the boundary layer, and the enhanced radial mixing between peripheral and core flows justify this result [11]. If scraping velocity increases ten times (ω=1), heat transfer augments only $Nu_{\omega=1}/Nu_{\omega=0.1}=1.55$. It reveals the fact that oscillatory flow mixing presents a saturation behaviour, owing to two opposite phenomena: during the counter-current semi-cycle, the flow structures that appear in the tube may promote intensive heat and mass transfer, and this effect should be as much important as the higher is the scraping velocity. However, during the co-current semi-cycle, the flow configuration may present low levels of enhanced heat transfer, according to the pressure drop signal (Figure 4) and the heat and momentum analogy [12]: the scraper movement in the flow direction generates low shear stress rates in the tube wall.

CONCLUSIONS

1. A comprehensive experimental research has been carried out to obtain the influence of scraping velocity on the thermal-hydraulic behaviour of a dynamic insert device, for low Reynolds number. The velocity ratio, ranging from 0.1 to 1, was found to be an excellent parameter to evaluate dynamic effects

2. The unsteady pressure evolution in the tube during the scraping cycle was assessed. Pressure drop in counter-current semi-cycle increases with scraping velocity, while it decreases during the co-current semi-cycle for higher scraping velocities.

3. Augmentations of pressure drop of 5.7 times were found for the device in static conditions, referred to a smooth tube with similar mass flow rate. Maximum increases of pressure drop of 1.2 times were found for ω=1, with respect to the static performance (ω=0).

4. Heat transfer increases of 4.1 times with respect to the smooth tube were found for the static device. The movement of the device promotes intensive heat and mass transfer, with augmentations of the order of 2 for ω=1, with respect to the static performance (ω=0).

ACKNOWLEDGMENTS

This research has been partially financed by the DPI2007-66551-C02-01 grant of the "Dirección General de Investigación del Ministerio de Educación y Ciencia de España" and the “HRS Spiratube” company.

REFERENCES

1. Webb, R.L., *Principles of Enhanced Heat Transfer,* Wiley Interscience, New York, 1994
2. Bergles, A.E., ExHFT for fourth generation heat transfer technology, *Experimental Thermal an Fluid Science,* Vol. 26, pp 335-344, 2002.
3. Müller-Steinhagen, H., *Handbook of Heat Exchanger Fouling – Mitigation and Cleaning Technologies*, Publico Publications, 2000.
4. Wang, W., Walt, J.H., McCarthy, K.L., Flow profiles of power law fluids in scraped surface heat exchanger geometry using MRI, *Journal of Food Process Engineering,* Vol. 22, pp 11-27, 1999.
5. De Goede, R., De Jong, E.J., Heat transfer properties of a scraped-surface heat exchanger in the turbulent flow regime, *Chemical Engineering Science,* Vol. 48, No. 8, pp.1393-1404, 1993.
6. Sun, K.-H., Pyle, D.L., Fitt, A.D., Please, C.P., Baines, M.J., Hall-Taylor, N., Numerical study of 2D heat transfer in a scraped surface heat exchanger, *Computers & Fluids,* Vol. 33 pp 869-880, 2004.
7. Solano, J.P., García, A., Pedrero, J.M., Vicente, P.G., Viedma, A., Experimental Investigation of flow pattern in enhanced heat exchangers with active insert devices, *Proceedings of ASME-ATI Conference,* Milan, Italy, May 2006, pp 252-260
8. Sieder, E.N., y Tate, E.G., Heat transfer and pressure drop of liquids in tubes, *Ind. Eng. Chem.,* Vol. 28, p. 1429. 1936.
9. Guide to the Expression of Uncertainty in Measurement, first ed., ISBN 92-67-10-188-9, *International Organization for Standardization,* Switzerland, 1995.
10. Vicente, P.G., García, A., Viedma, A., Experimental study of mixed convection and pressure drop in helically dimpled tubes for laminar and transition flow, *International Journal of Heat and Mass Transfer,* Vol. 45, pp 5091–5105, 2002.
11. Mackley, M.R., Stonestreet, P., Heat transfer and associated energy dissipation for oscillatory flow in baffled tubes, *Chemical Engineering Science,* Vol. 50 (14), pp 2211-2224, 1995.
12. Colburn, A.P., A method of correlating forced convection heat transfer data and a comparison with fluid friction, *Trans. AIChE,* Vol. 29, 174-210, 1933.